

Semantic-Guided Generative Image Augmentation Method with Diffusion Models for Image Classification

Bohan Li, Xiao Xu, Xinghao Wang, Yutai Hou, Yunlong Feng, Feng Wang, Xuanliang Zhang, Qingfu Zhu*, Wanxiang Che

Harbin Institute of Technology, Harbin, China

{bhli, xxu, xhwang, ythou, ylfeng}@ir.hit.edu.cn, {7203610216, 1201020412}@stu.hit.edu.cn, {qfzhu, car}@ir.hit.edu.cn

Abstract

Existing image augmentation methods consist of two categories: perturbation-based methods and generative methods. Perturbation-based methods apply pre-defined perturbations to augment an original image, but only locally vary the image, thus lacking image diversity. In contrast, generative methods bring more image diversity in the augmented images but may not preserve semantic consistency, thus may incorrectly changing the essential semantics of the original image. To balance image diversity and semantic consistency in augmented images, we propose **SGID**, a Semantic-guided Generative Image augmentation method with Diffusion models for image classification. Specifically, SGID employs diffusion models to generate augmented images with good image diversity. More importantly, SGID takes image labels and captions as guidance to maintain semantic consistency between the augmented and original images. Experimental results show that SGID outperforms the best augmentation baseline by 1.72% on ResNet-50 (from scratch), 0.33% on ViT (ImageNet-21k), and 0.14% on CLIP-ViT (LAION-2B). Moreover, SGID can be combined with other image augmentation baselines and further improves the overall performance. We demonstrate the semantic consistency and image diversity of SGID through quantitative human and automated evaluations, as well as qualitative case studies.

1 Introduction

The data-hungry problem in deep learning has been a hot topic (Minaee et al. 2021) since a sufficient number of training samples is crucial for unleashing the power of deep networks (Zhang et al. 2022). However, manually collecting and labeling large-scale datasets are both expensive and time-consuming (Li, Hou, and Che 2022), giving rise to the Data Augmentation (DA) methods. Take image classification as an example, generally, a DA method generates augmented images that are diverse from the original training images while preserving the essential semantics of the original images. It has been demonstrated to be effective in improving the model performance on classification tasks in practice (Dunlap et al. 2023).

Typically, DA methods for image classification can be divided into two categories: perturbation-based and

Image	ViT (ImageNet-21k)	More Semantic Consistency ←			→ More Image Diversity	
		CutMix	RA	SGID	SGID+DC	Text2Img
Call101	91.20	91.77 (+0.57)	91.92 (+0.72)	93.91 (+2.71)	93.44 (+2.24)	91.21 (+0.01)
Cars	82.99	84.20 (+1.21)	85.62 (+2.63)	86.73 (+3.74)	86.33 (+3.34)	85.81 (+2.82)
Flowers	95.70	96.53 (+0.83)	96.66 (+0.96)	97.16 (+1.46)	97.12 (+1.42)	96.93 (+1.23)
DTD	71.22	71.32 (+0.10)	71.32 (+0.10)	73.35 (+2.13)	72.30 (+1.08)	70.57 (-0.65)
Avg.	85.28	85.96 (+0.68)	86.38 (+1.10)	87.79 (+2.51)	87.30 (+2.02)	86.13 (+0.85)

Figure 1: A comparison of four baseline methods and our proposed SGID using the ViT (ImageNet-21k) backbone across four datasets. Our SGID strikes a balance between semantic consistency and image diversity, leading to the highest performance improvement.

generation-based. The former obtains augmented images by modifying the original image with pre-defined perturbations, e.g., image erasing (Zhong et al. 2020) and image mixup (Yun et al. 2019). In this way, most of the semantics remain since the augmented image only locally differs from the original image in a limited area. However, the diversity is quite limited at the same time and becomes the bottleneck of the methods of this category. In contrast, the generation-based methods synthesize augmented images by generative models like diffusion models (Rombach et al. 2022). They directly generate augmented images based on label-related captions and/or original images. In this way, they can generate quite diverse images but is inferior to the perturbation-based methods in preserving semantics, which are less diverse but more semantically consistent. The excessive noise or diversity introduced by generative DA methods may **incorrectly change** the essential semantics of the original image. As shown in Figure 1, the last two augmented images incorrectly show two door handles on the same side of the door or change the badge on the rear of the car.

Naturally, we intend to explore how to maintain a bal-

*Corresponding Authors.

ance between image diversity and semantic consistency in a generative image DA method, which has not yet been systematically explored by existing methods, to achieve better performance on image classification tasks. To this end, we propose SGID, a **Semantic-guided Generative Image** augmentation method with **D**iffusion models for image classification. It ensures semantic consistency between the original and augmented images, and achieves good image diversity (see Figure 1). SGID consists of two steps: **(1)** Collect the text label of the image and then generate the image caption with the BLIP (Li et al. 2022) model. Both of them convey the essential semantics of the original image. **(2)** Concatenate the label and caption to construct a textual prompt and subsequently feed it into the Stable Diffusion (Rom-bach et al. 2022) model along with the original image. SGID tends to generate diverse augmented images, while the textual prompt as semantic guidance help to preserve the essential semantics of the original images (see Sec 4.4).

We conduct experiments on seven image classification datasets based on three backbones including ResNet-50 (from scratch) (He et al. 2016), ViT (ImageNet-21k) (Dosovitskiy et al. 2020), and CLIP-ViT (LAION-2B) (Cherti et al. 2022). We compare SGID with seven strong DA baselines including four perturbation-based methods and three generative methods. Our method outperforms the backbones on all datasets and achieves the best or comparable performance to all baselines. Especially, SGID leads to 10.39%, 2.08%, 0.85% average accuracy gain across three backbones and seven datasets, respectively. Moreover, we find that combining SGID with standard DA baselines can achieve further improvement on seven datasets. We further compare the semantic consistency and diversity between SGID as well as baselines by human evaluation, automatic similarity evaluation, and case studies.

Our contributions are as follows:

- We propose a **Semantic-guided Generative Image** augmentation method with **D**iffusion models (SGID) for image classification. Human evaluation, automated evaluations, and case studies demonstrate that SGID balances the semantic consistency and image diversity.
- SGID achieves better average performance than the best baseline by 1.72%, 0.33%, and 0.14% across three backbones and seven datasets.
- SGID can be combined with other image augmentation baselines and further improves the overall performance.

2 Background

Image augmentation is widely used in computer vision (Minaee et al. 2021; Algan and Ulusoy 2021). It generates augmented images that are diverse from the original images while preserving their semantics. Common augmentation methods include **(1)** perturbation-based methods and **(2)** generative methods.

Perturbation-based methods apply pre-defined perturbations to augment an original image and preserve image semantic consistency (Yang et al. 2022). *Random Erasing* (Zhong et al. 2020) generates augmented images by deleting one or more subregions of an image. *CutMix* (Yun et al. 2019) uses the full or partial features and labels

of different images to apply some interpolation methods. *RandAugment* (Cubuk et al. 2020) tries to search the space of augmentation methods according to different tasks. *MoEx* (Li et al. 2021) performs the transformation in a learned feature space rather than conducting augmentation only in the input space. Despite their effectiveness in image classification, the pre-defined perturbations of these methods only locally vary the images, thus lacking diversity.

Thanks to the development of generative models like Stable Diffusion (SD), an image generation model pre-trained on large-scale image-text pairs, there are some attempts at generative methods for more diversity (Zhang et al. 2022). *Text2Img* (He et al. 2022) applies a fine-tuned T5 model to generate captions based on image labels, and then employs a text-to-image diffusion model to generate images without using the original image. Dunlap et al. (2023) respectively use diverse captions or editing instructions to modify original images into augmented images. During image generation, they correspondingly employ the Image2Image diffusion model or the InstructPix2Pix diffusion model (Brooks, Holynski, and Efros 2023) as generative models. Inspired by this work, we take its spirit into our SGID to obtain two variants of SGID as generative baselines named *SGID+DiverseCaption* and *SGID+InstructPix2Pix*.¹

However, existing generative methods may incorrectly change the essential semantics of the original image, which is crucial for image classification (Burg et al. 2023).

This paper aims to improve the semantic consistency of generative methods through guiding the generation of augmented images by explicitly using the essential semantics of original images. SGID balances the image diversity and semantic consistency in augmented images, and achieves consistent performance gains across datasets and backbones.

3 SGID

In this paper, we propose SGID, a semantic-guided generative image augmentation method with diffusion models for image classification. We do not aim to exceed existing image augmentation baselines on various datasets and different backbones, but to explore such a method that balances image diversity and semantic consistency, *i.e.*, preserving the essential semantics of the original images and simultaneously bringing good image diversity. In addition, SGID can be naturally combined with other DA baselines and further improve their performance. It consists of two essential steps, as illustrated in Figure 2:

1. We first collect textual labels for each image, then use BLIP to generate captions, and then use CLIP (Radford et al. 2021) to calculate the similarity between the chosen caption and the original image. Both labels and captions provide the essential semantics of the original images.
2. We construct the prompt based on the label and the caption of each image. The prompt is subsequently fed into Stable Diffusion along with the original image. The semantic guidance contained in the prompt can help gener-

¹We further discuss this work (Dunlap et al. 2023) and other generative methods in Appendix Sec. G and D.

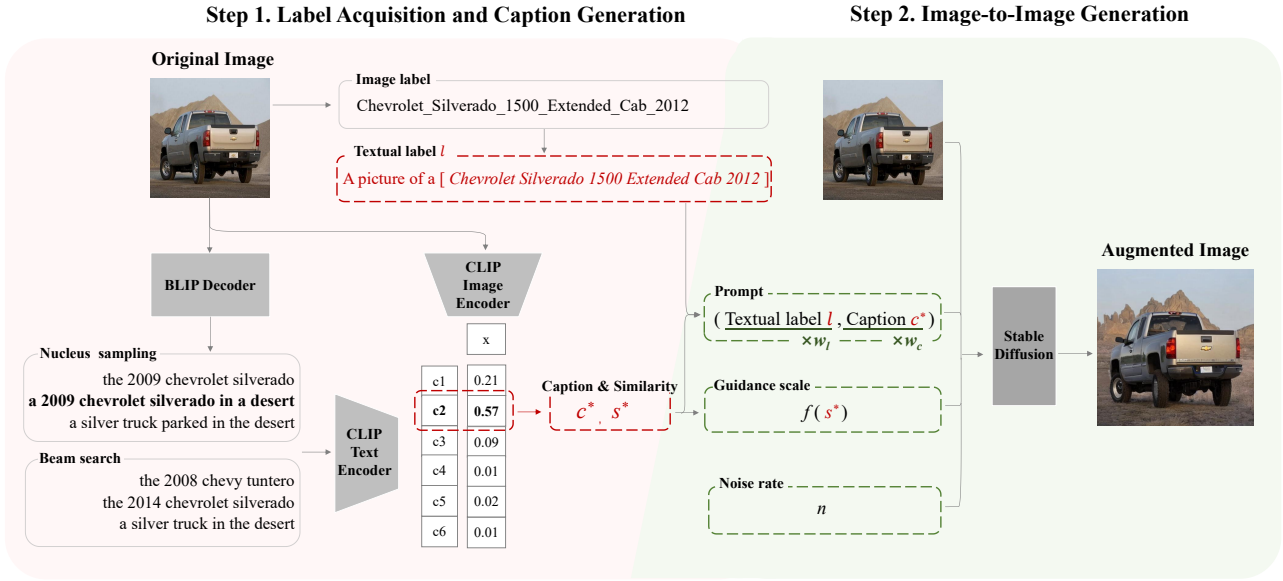


Figure 2: An illustration of our **SGID**. **Step 1** first collects textual labels for each image, then use BLIP to generate captions, and then use CLIP to calculate the similarity between the chosen caption and the original image. **Step 2** generates the augmented images through the Stable Diffusion model, utilizing the original image, the prompt consisting of the textual label and caption, the noise rate, and the guidance scale based on the similarity.

ate diverse and semantic-consistent augmented images.²

3.1 Label Acquisition and Caption Generation

In **Step 1**, we construct prompts from original images as semantic guidance for the subsequent **Step 2**. The prompt consists of the textual label and the caption of the original image. We argue that the image label contains accurate semantic information and the caption provides the overall description of the image. Thus, the prompt is an explicit constraint to preserve semantic consistency. Specifically, for each image $x \in \mathcal{X}$ in an image classification dataset $\mathcal{D} = (\mathcal{X}, \mathcal{Y})$, we first employ its groundtruth image label to construct a corresponding sentence as the textual label l :

$$l = \text{“A picture of a [label]”}. \quad (1)$$

Then we generate captions for the image by the BLIP model:

$$c = \text{BLIP}(x). \quad (2)$$

We explore different sampling strategies, including beam search (Shen et al. 2017) and nucleus sampling (Holtzman et al. 2019)). Beam search tends to generate common and safe captions, hence offering less extra knowledge, and Nucleus sampling generates more diverse captions (Li et al. 2022). We choose one of the sampling strategies based on the results of the validation set. For each image, we obtain the corresponding caption set $\mathcal{C} = \{c_1, c_2, \dots, c_k\}$ and randomly select one caption from it. Captions can provide further semantic information beyond the object category of the image, such as the description of the background and

color. Combining captions with groundtruth but often too-short image labels can provide effective semantic guidance for image-to-image generation.

Moreover, to increase the semantic consistency of the prompt, we also explore potentially higher-quality captions by taking CLIP as an **optional** filter. Given the generated caption set \mathcal{C} , we use CLIP to calculate the similarity between the original image with each caption and obtain the similarity set: $\mathcal{S} = \{s_1, s_2, \dots, s_k\}$. We select the caption with the highest similarity in \mathcal{S} . We denote the selected caption and its similarity with c^* and s^* . For example, in Figure 2, the caption $c^* = \text{“a 2009 chevrolet silverado in a desert”}$ generated by nucleus sampling gets the highest similarity $s^* = 0.57$.

3.2 Image-To-Image Generation

In **Step 2**, we take the textual label l and the caption c^* as semantic guidance for image-to-image generation. We first concatenate l and c^* to construct the *textual prompt*, i.e., $p = (l, c^*)$. For example, “A picture of a [Chevrolet Silverado 1500 Extended Cab 2012], a 2009 chevrolet silverado in a desert.” in Figure 2. The textual prompt carries not only accurate but brief image semantics from l , but also the overall image description from c^* . It serves as a part of the input to Stable Diffusion to provide semantic guidance for augmented image generation. As for image diversity, we apply Gaussian noise with a noise rate n in Stable Diffusion to make slight changes to the original image based on the above semantic constraint.

Considering the different contributions of l and c^* to p , we adopt the **prompt weighting** strategy. Specifically, we apply different weights w_l, w_c for the label and caption re-

²The introduction to BLIP, CLIP, and SD is Appendix Sec. E.

	CIFAR-100	CIFAR-10	Cal101	Cars	Flowers	Pets	DTD	Avg.	
ResNet-50 (from scratch)	Backbone (He et al. 2016)	75.12	94.81	47.38	82.26	33.02	50.30	19.85	57.53
	+ Random Erasing (Zhong et al. 2020)	76.35	95.34	46.26	80.73	34.62	49.30	20.65	57.61
	+ CutMix (Yun et al. 2019)	77.56	95.52	49.28	83.55	33.35	51.21	20.14	58.66
	+ MoEx (Li et al. 2021)	76.00	95.23	52.74	81.13	36.27	55.79	21.20	59.77
	+ RandAugment (Cubuk et al. 2020)	76.40	95.00	58.55	86.85	41.97	57.45	25.02	63.03
	+ Text2Img (He et al. 2022)	74.99	94.97	57.60	85.44	42.06	67.08	31.18	64.76
	+ SGID (Ours)	75.72	95.48	59.17*	88.53*	45.61*	73.71*	37.19*	67.92*
	+ DiverseCaption (Dunlap et al. 2023)	75.14	95.10	58.29	87.86	43.66	69.73	33.61	66.20
	+ InstructPix2Pix (Dunlap et al. 2023)	75.09	94.70	56.83	86.32	42.30	68.14	30.22	64.80
	+ SGID & MoEx	77.54	<u>95.68</u>	<u>70.56</u>	87.33	<u>49.20</u>	<u>76.52</u>	<u>38.92</u>	<u>70.82</u>
	+ SGID & RandAugment	77.56	<u>95.49</u>	75.94	91.07	55.71	82.98	49.78	75.50
	+ Text2Img & SGID	75.40	95.06	64.20	87.94	42.36	69.28	35.79	67.15
ViT (ImageNet-21k)	Backbone (Dosovitskiy et al. 2020)	89.86	98.61	91.20	82.99	95.70	92.04	71.22	88.80
	+ Random Erasing (Zhong et al. 2020)	89.87	98.67	91.71	83.94	96.28	92.55	72.07	89.30
	+ CutMix (Yun et al. 2019)	89.94	98.67	91.77	84.20	96.53	92.45	71.32	89.27
	+ MoEx (Li et al. 2021)	90.11	98.67	92.24	85.94	96.78	92.66	70.79	89.60
	+ RandAugment (Cubuk et al. 2020)	90.32	98.60	91.92	85.62	96.66	92.91	71.32	89.62
	+ Text2Img (He et al. 2022)	92.66	99.01	91.21	85.81	96.93	92.67	70.57	89.84
	+ SGID (Ours)	92.66	98.96	93.91*	86.73*	97.16*	93.38	73.35*	90.88*
	+ DiverseCaption (Dunlap et al. 2023)	92.59	98.66	93.44	86.33	97.12	93.38	72.30	90.55
	+ InstructPix2Pix (Dunlap et al. 2023)	92.53	98.50	92.19	85.82	97.04	<u>93.02</u>	71.70	90.11
	+ SGID & MoEx	92.02	<u>98.83</u>	<u>94.00</u>	<u>87.80</u>	96.69	92.99	<u>73.45</u>	<u>90.83</u>
	+ SGID & RandAugment	91.64	98.72	94.30	88.28	<u>97.13</u>	94.00	74.14	91.17
	+ Text2Img & SGID	92.69	99.03	91.35	85.84	97.17	<u>93.30</u>	71.27	90.09
CLIP-ViT (LAION-2B)	Backbone (Cherti et al. 2022)	85.89	95.04	92.96	85.13	91.46	93.69	65.81	87.14
	+ Random Erasing (Zhong et al. 2020)	86.26	95.27	<u>94.32</u>	85.26	91.53	93.88	66.33	87.55
	+ CutMix (Yun et al. 2019)	85.98	95.20	93.85	85.43	91.64	94.01	66.20	87.47
	+ MoEx (Li et al. 2021)	86.02	95.16	93.81	85.79	91.97	93.76	67.18	87.67
	+ RandAugment (Cubuk et al. 2020)	86.08	95.32	93.79	86.84	91.88	93.95	66.74	87.80
	+ Text2Img (He et al. 2022)	85.80	94.77	93.72	86.80	91.90	93.71	64.50	87.31
	+ SGID (Ours)	86.53*	95.66*	94.29	87.19*	92.04*	93.98	66.25	87.99*
	+ DiverseCaption (Dunlap et al. 2023)	86.07	95.44	94.33	87.12	92.01	93.97	66.04	87.85
	+ InstructPix2Pix (Dunlap et al. 2023)	86.13	95.20	93.88	87.06	91.93	93.92	66.00	87.73
	+ SGID & MoEx	86.59	<u>95.42</u>	<u>93.88</u>	86.34	<u>92.05</u>	94.19	67.51	88.00
	+ SGID & RandAugment	86.66	95.68	94.52	88.06	92.75	<u>94.13</u>	<u>67.45</u>	88.46
	+ Text2Img & SGID	85.87	95.16	93.76	86.93	92.04	93.74	64.63	87.45

Table 1: Accuracy of seven image classification datasets and three backbones by four baselines. On each backbone, the performance of the backbones, the perturbation-based methods, the generative methods (including **SGID**), the integrated methods are provided. The best and second best results in the DA method and integrated methods for each dataset are **bolded** and underlined. The numbers with * indicate that the improvement of SGID is statistically significant with $p < 0.05$ under t-test.

spectively by multiplying the token embeddings of l and c^* by w_l and w_c respectively. Furthermore, to control the extent of semantic guidance on image generation, we adopt the **guidance mapping** strategy that provides a *proper* guidance scale g . The guidance scale g control how much the image generation process follows the semantic guidance, *i.e.*, the textual prompt p . We apply a function f to map the similarity s^* between the original image x and the chosen caption c^* , to the guidance scale $g = f(s^*)$. Finally, Stable Diffusion generates the augmented images given the above elements:

$$x' = \text{StableDiffusion}(x, p, g, n), \quad (3)$$

where x, x' is the original and augmented image, p is the textual prompt, g is the guidance scale, and n is the noise rate.

4 Experiments

4.1 Experimental Settings

Datasets: We evaluate the effectiveness of our proposed method on seven commonly used datasets, including three *coarse-grained* object classification datasets: CIFAR-10,

CIFAR-100 (Krizhevsky 2009), Caltech101 (Cal101) (Fei-Fei, Fergus, and Perona 2004), and four *fine-grained* object classification datasets: Stanford Cars (Cars) (Krause et al. 2013), Flowers102 (Flowers) (Nilsback and Zisserman 2008), OxfordPets (Pets) (Parkhi et al. 2012) and texture classification DTD (Cimpoi et al. 2014).

Backbones: We conduct experiments on three backbones, including a basic model from scratch: ResNet-50 (from scratch) (He et al. 2016), and two pre-trained models: ViT (ImageNet-21k) (Dosovitskiy et al. 2020), CLIP-ViT (LAION-2B) (Cherti et al. 2022). Specifically, ViT (ImageNet-21k) is supervised trained on ImageNet-21k, while CLIP-ViT (LAION-2B) is self-supervised pre-trained on the CLIP paradigm on almost the same pre-trained corpus as the image generation model Stable Diffusion (SD).³

Baselines: We apply various DA methods introduced in Sec. 2 as baselines, including four perturbation-based methods: *Random Erasing* (RE), *CutMix*, *MoEx*, and *RandAugment* (RA), and three generative meth-

³For more details of CLIP-ViT (LAION-2B), see Appendix Sec. I

ods: *Text2Img*, *SGID+DiverseCaption* (*SGID+DC*), and *SGID+InstructPix2Pix* (*SGID+IP*). All generative methods employ the same image generation model SD. we re-implement *Text2Img*, *SGID+DC*, and *SGID+IP* to provide extensive experiments across datasets and backbones.

4.2 Implementation Details

We apply nucleus sampling and beam search to respectively generate 10 captions by BLIP. The caption length is between 5 and 20. We use $p = 0.9$ by default in nucleus sampling and $num_beams = 3$ by default in beam search. The default “CLIP-ViT-B/32” model is used for calculating image-text similarity. We apply the pre-trained “stable-diffusion-v1-5” model and generate one augmented image for each original image.⁴ Empirically, we take $f(s^*) = -4 \cdot (s^*)^2 + 2 \cdot s^* + 1$ as the guidance mapping function. We select the noise rate n from $\{0.3, 0.5, 0.7\}$.⁵ As for prompt weighting, We assign a weight of 1.50 to the labels because it carries more accurate information for the original image, and a weight of 0.90 to the caption to reduce the interference caused by the potential low-quality captions. We run each method over 5 different random seeds. See Appendix Sec. I for more details including the training of image classifiers.⁶

4.3 Main Results

In this paper, we conduct experiments on three backbones with seven strong DA baselines on seven datasets. Our analysis of these results is based on three perspectives: (1) overall performance on three backbones; (2) average performance gain compared to the best baselines; (3) average performance gain for combined models. We believe the significant performance gain across the above backbones, datasets, and baselines demonstrates the effectiveness and generalizability of SGID. Our main results are shown in Table 1 and Appendix Sec. C.

For (1), overall, SGID shows positive effects and achieves the highest performance on average across all seven datasets and three backbones. Specifically, our method leads to 10.39% accuracy gains on ResNet-50 (from scratch), 2.08% on ViT (ImageNet-21k), and 0.85% on CLIP-ViT (LAION-2B). This demonstrates that augmenting images with semantic guidance to diffusion models can benefit different backbones. Notably, SGID still shows improvement on CLIP-ViT (LAION-2B), whose pre-training data is almost identical to SD. This demonstrates the effectiveness of the paradigm introduced in SGID: preserving **semantic consistency** in original images and simultaneously bringing good **image diversity**, which will be further discussed in Sec. 4.4.

For (2), with semantic guidance, SGID performs comparably or better than the best perturbation-based and generative baselines. Specifically, SGID outperforms *RandAug-*

⁴SD v1-5 is mainly pre-trained on LAION-2B (Schuhmann et al. 2022).

⁵The larger n brings more variation. We choose $n \in [0, 1]$ from $\{0.3, 0.5, 0.7\}$ to preserve image semantics and bring explicit changes in the background, position, etc.

⁶Our code will be released at <https://github.com/BohanLi0110/SGID>

	Cal101		DTD		Pets		Avg.		Avg. Performance
	Con.	Div.	Con.	Div.	Con.	Div.	Con.	Div.	
RandAugment	4.49	1.30	4.51	1.50	4.70	1.34	4.57	1.38	63.03
SGID	4.07	1.99	4.40	1.76	4.52	1.98	4.33	1.91	67.92
SGID+DC	3.56	2.33	3.33	2.71	3.76	2.58	3.55	2.54	<u>66.20</u>
Text2Img	1.67	4.56	1.27	4.87	1.41	4.62	1.45	4.68	64.76

Table 2: Human evaluation results of four DA methods on three datasets from the perspectives of semantic consistency (Con.) and Diversity (Div.). “SGID+DC” indicates SGID+DiverseCaption.

ment and *SGID+DiverseCaption* by 4.89% and 1.72% on average on ResNet-50 (from scratch), by 1.26% and 0.33% on ViT (ImageNet-21k), and by 0.19% and 0.14% on CLIP-ViT (LAION-2B). Higher performance than four strong baselines shows promising capabilities of SGID to generate images with diffusion models under semantic guidance, *i.e.*, balancing diversity and semantic consistency.

For (3), SGID can be combined with perturbation-based and generative baselines for further improvement. We separately explore applying RandAugment based on SGID and applying SGID based on Text2Img.⁷ We find the above integrated methods achieve further improvements, and this conclusion holds on three backbones. For example, as a combination of “perturbation-based & generation-based”, “SGID & RA” exceeds RA on three backbones by 12.47%, 1.55% and 0.66%, and exceeds SGID by 7.58%, 0.29% and 0.47%. Consistent and significant performance gains further prove our SGID not only preserves the essential semantics of the original images while bringing good diversity, but also benefits mutually with the perturbation-based method. Interestingly, although “generation-based” methods, *Text2Img* and our SGID, share the same image generation model, “Text2Img & SGID” still achieves performance gains compared with *Text2Img* (2.39%, 0.25% and 0.14%), but underperforms SGID (−0.77%, −0.79% and −0.54%). We attribute the gains to the semantic guidance introduced by our SGID, but attribute the reductions to the fact that *Text2Img* may incorrectly change the essential semantics of original images.

4.4 Image Diversity and Semantic Consistency

In this section, we aim to discuss the image diversity and semantic consistency of SGID and other baselines from three perspectives: (1) human evaluation; (2) automatic similarity evaluation; (3) case study. We try to analyze the potential reason why SGID achieves better performance than existing perturbation-based baselines and generative methods.

Human Evaluation We apply human evaluation on one coarse-grained object classification dataset (Caltech101), one fine-grained object classification dataset (OxfordPets),

⁷Applying RandAugment based on SGID” indicates conducting the RandAugment transformation based on the augmented images of SGID. “Applying SGID based on Text2Img” indicates conducting SGID based on the augmented images of Text2Img. We provide more results of combined models in Appendix Sec. A.

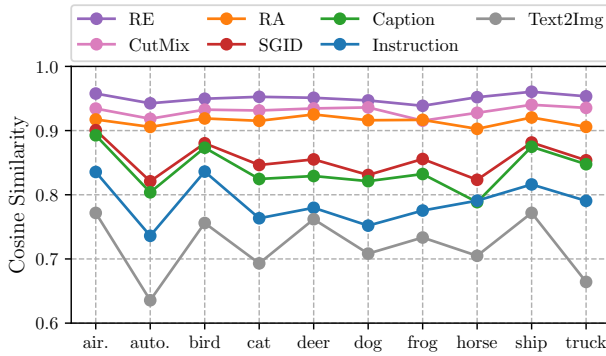


Figure 3: Average cosine similarity between the augmented and original images for each category of CIFAR-10 (air.: airplane, auto.: automobile).

and the texture classification dataset (DTD).⁸ For each dataset, we randomly choose 10 labels and 10 of their corresponding original images. We compare SGID with the best perturbation-based and generative baselines: RandAugment, Text2Img, and SGID+DiverseCaption. We evaluate the augmented images by four DA methods based on the original image. Each augmented image is scored on a scale of 1 ~ 5 in terms of image diversity and semantic consistency respectively. We employ three experienced annotators. The annotators are trained and pass trial annotations. Each annotator spends an average of 4.5 hours on annotation, and the salary for labeling each piece of data is \$1. Table 2 shows the human evaluation results for four methods and their corresponding average performance on ResNet-50 (from scratch).

We can find that SGID has similar semantic consistency and more image diversity than RandAugment, but more semantic consistency and less image diversity than Text2Img and SGID+DiverseCaption. When both image classification performance and human evaluation results are considered, our SGID achieves the best performance by balancing image diversity and semantic consistency through semantic-guided generative image augmentation.

Automatic Similarity Evaluation We choose CIFAR-10 for automatic similarity evaluation and separately use SGID and six DA baselines to generate five augmented images for each original image.⁹ For each DA method, we calculate the average cosine similarity between the original image and its five augmented ones (Zhang et al. 2022). We repeat this process on all original images and calculate the average value for each label as a measure of diversity. The lower the average similarity between the augmented images and the original image, the lower the semantic consistency but the more significant the diversity brought by the corresponding DA method. The results are shown in Figure 3.

Overall, SGID has a lower similarity (0.8548) compared to perturbation-based DA methods, while it has a higher sim-

⁸The image size of CIFAR-10 and CIFAR-100 are $32 * 32$, which is too small for human evaluation.

⁹We do not include MoEx since it performs the transformation in an implicit feature space instead of the explicit input space.

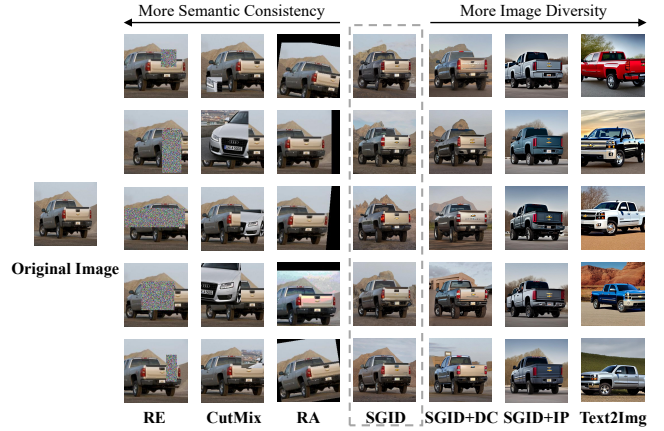


Figure 4: Case study of seven DA methods.

ilarity compared to other generative methods. The average similarity of our SGID is between the two categories of DA methods, but SGID performs best in the image classification task. This further demonstrates the significance of balancing image diversity and semantic consistency.

Case Study Figure 4 compares the augmented images generated by SGID and the other six baselines.¹⁰ The three perturbation-based methods bring diversity through transformations. However, these pre-defined transformations could not provide sufficient diversity for augmented images. Generative baselines bring more diverse and vivid images than perturbation-based baselines, but they struggle to preserve the semantic consistency of original images. In contrast, SGID preserves the semantic consistency from original images and provides good image diversity, which also results in a performance improvement in downstream tasks.

4.5 Ablation Study

In this section, we study the influence of some essential components in SGID, including (1) the construction of the textual prompt; (2) the caption filter and the prompt weighting; (3) the noise rate and the guidance scale. We further explore augmented image filtering in Appendix Sec. B.

Influence of Textual Prompts We study the influence of textual prompts based on ResNet-50 (from scratch) across four datasets in Table 3. We have the following conclusions: (i) The semantic guidance is important for the image-to-image paradigm in SGID. In most cases, *i.e.*, *Cars*, *Pets*, and *DTD*, the performance of “w/o Prompt” is the lowest. This means that semantic guidance is essential for image augmentation to preserve semantic consistency. (ii) The label and the caption both provide semantic constraints. In most cases except for *Cars*, “+ Complete Prompt” shows the best results. As for *Cars*, “+ Label Only” has higher performance than “+ Complete Prompt”. We attribute that the dataset is fine-grained and its labels carry very detailed information like “Chevrolet_Silverado_1500_Extended_Cab_2012”,

¹⁰More case studies are in Appendix Figure 8 - Figure 13.

	CIFAR-100	Cars	Pets	DTD
w/o Prompt	74.11	82.09	55.76	32.39
+ Caption Only	75.65	83.89	63.80	34.78
+ Label Only	73.99	88.53	75.90	37.43
+ Complete Prompt	75.72	84.31	76.15	37.55

Table 3: Ablation study of textual prompts. “w/o Prompt” indicates no semantic guidance, “+ Caption Only”, “+ Label Only”, and “Complete Prompt” use the caption only, the label only, and the complete prompt as the guidance.

	CIFAR-100		Pets		DTD	
	PW	w/o PW	PW	w/o PW	PW	w/o PW
Beam	75.60	74.69	75.06	76.15	37.47	35.79
Nucleus	75.72	74.93	73.72	75.70	37.16	37.04
Caption Filter	74.80	74.85	70.86	71.95	37.55	32.44

Table 4: Ablation study of caption sampling and prompt weighting. “Caption Filter” indicates using CLIP to choose the caption with the highest similarity to the original image among the 20 captions generated by “Beam” and “Nucleus”. “PW” indicates the prompt weighting strategy.

which is sufficient for the PMs to generate an augmented image based on the original one. However, BLIP struggles to generate fine-grained captions, thus the generated captions have a counterproductive effect. (iii) In most cases, “+ Label Only” outperforms “+ Caption Only” since the image label carries groundtruth and accurate image semantics. However, for *CIFAR-100*, “+ Caption Only” shows a better result than “+ Label Only”. We attribute to the short label, e.g., bed, forest, etc., provided by *CIFAR-100* cannot provide detailed information in the label like other fine-grained datasets.

Caption Sampling & Prompt Weighting We study the influence of caption sampling and prompt weighting based on ResNet-50 (from scratch) in Table 4. Nucleus sampling, beam search, and the caption filter contribute the best performance on the three datasets respectively. This may be because of the different characteristics of nucleus sampling and beam search, as mentioned in Section 3.2. Nucleus sampling generates more diverse and surprising captions, while beam search tends to generate safe captions (Li et al. 2022). We hypothesize that *Pets* is a fine-grained dataset whose labels are very detailed and a “safe” caption would not influence the semantics of the labels. In contrast, short labels in *CIFAR-100* cannot convey sufficient semantics, thus more diverse captions from nucleus sampling are required. *DTD*, the texture classification dataset, is challenging for BLIP to generate captions ensuring image semantics. Then the caption filter would help to improve caption quality for semantic consistency. As for prompt weighting, its effectiveness is proven in two out of three datasets. We hypothesize that adding different weights to the label and the caption could reconcile their different semantic information.

Influence of Noise Rate and Guidance Scale. We further explore the effect of adjusting the noise rate and guidance scale on generating augmented images. As shown in Figure 5(b), the generated images show more diversity (e.g., varia-

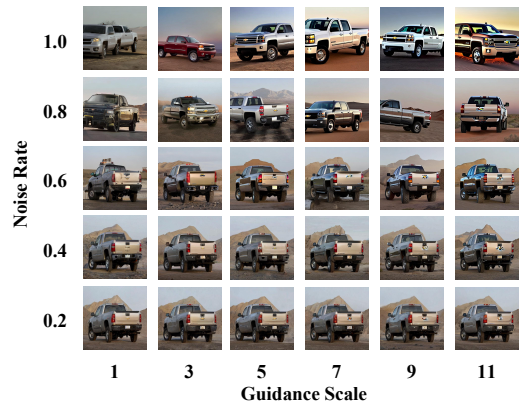


Figure 5: Case study on the influence of noise rate and guidance scale when generating images by SGID on Cars.

tions in body orientation, color, background, etc.) when the noise rate and the guidance scale are increased. However, the experimental results show that as the noise rate increases, the performance decreases while more diversity is introduced. This suggests that noise rate has a great effect on performance and deserves further exploration in future work.

5 Related Works

Diffusion Model-Based Methods. There are some works employing diffusion models to generate augmented images or expand datasets. Zhang et al. (2022), He et al. (2022), and Dunlap et al. (2023) generate images based on label-related constraints and/or original images. Li et al. (2023) and Shipard et al. (2023) generate samples for training zero-shot classifiers without relying on original images. While acknowledging the importance of zero-shot learning, this paper focuses on linear probing to improve model performance in image classification. Akrouf et al. (2023), Carlini et al. (2023), and Bakhtiarnia, Zhang, and Iosifidis (2023) apply diffusion models for DA in other tasks like skin disease classification, privacy attacks, and crowd counting. These are promising directions we would explore in the future.

Knowledge Distillation (KD). There have been some works using PMs to generate training data (Meng et al. 2022; Wang et al. 2021a) and referring to it as a variant of KD (Ye et al. 2022). To some extent, our work could also be categorized as KD. Semantic-guided image generation via pre-trained diffusion models can be seen as a more straightforward and effective form to precisely distill knowledge from pre-trained diffusion models. Moreover, it can be naturally combined with the traditional KD as a new direction.

6 Conclusion

In this paper, we introduce **SGID**, a **S**emantic-guided **G**enerative **I**mage augmentation method with **D**iffusion models for image classification. The proposed method balances image diversity and semantic consistency. Specifically, SGID constructs prompts with image labels and captions as semantic guidance to generate augmented images

that preserve the essential semantics in original images and simultaneously bring good image diversity. We demonstrate the effectiveness of SGID by experiments on three backbones with seven strong image augmentation baselines on seven different datasets and SGID outperforms the backbones on all datasets and achieves the best or comparable performance to all baselines. Moreover, SGID can be combined with other image augmentation baselines and further improves the overall performance. We also evaluate the semantic consistency and image diversity of SGID through quantitative human and automated evaluations, as well as qualitative case studies.

Acknowledgments

We gratefully acknowledge the support of the National Natural Science Foundation of China (NSFC) via grant 62236004 and 62206078, and the support of Du Xiaoman (Beijing) Science Technology Co., Ltd.

References

- Akrouf, M.; Gyepesi, B.; Holló, P.; Poór, A. K.; Kincso, B.; Solis, S.; Cirone, K. D.; Kawahara, J.; Slade, D.; Abid, L.; Kovács, M.; and Fazekas, I. 2023. Diffusion-based Data Augmentation for Skin Disease Classification: Impact Across Original Medical Datasets to Fully Synthetic Images. *ArXiv*, abs/2301.04802.
- Algan, G.; and Ulusoy, I. 2021. Image classification with deep learning in the presence of noisy labels: A survey. *Knowledge-Based Systems*.
- Bakhtiarnia, A.; Zhang, Q.; and Iosifidis, A. 2023. Prompt-Mix: Text-to-image diffusion models enhance the performance of lightweight networks. *ArXiv*, abs/2301.12914.
- Brooks, T.; Holynski, A.; and Efros, A. A. 2023. Instruct-Pix2Pix: Learning to Follow Image Editing Instructions. *arXiv:2211.09800*.
- Burg, M. F.; Wenzel, F.; Zietlow, D.; Horn, M.; Makansi, O.; Locatello, F.; and Russell, C. 2023. A data augmentation perspective on diffusion models and retrieval. *ArXiv*, abs/2304.10253.
- Carlini, N.; Hayes, J.; Nasr, M.; Jagielski, M.; Sehwag, V.; Tramèr, F.; Balle, B.; Ippolito, D.; and Wallace, E. 2023. Extracting Training Data from Diffusion Models. *ArXiv*, abs/2301.13188.
- Changpinyo, S.; Sharma, P.; Ding, N.; and Soricut, R. 2021. Conceptual 12m: Pushing web-scale image-text pre-training to recognize long-tail visual concepts. In *Proc. of CVPR*.
- Cherti, M.; Beaumont, R.; Wightman, R.; Wortsman, M.; Ilharco, G.; Gordon, C.; Schuhmann, C.; Schmidt, L.; and Jitsev, J. 2022. Reproducible scaling laws for contrastive language-image learning. *ArXiv*, abs/2212.07143.
- Cho, J.; Lei, J.; Tan, H.; and Bansal, M. 2021. Unifying vision-and-language tasks via text generation. In *Proc. of ICML*.
- Cimpoi, M.; Maji, S.; Kokkinos, I.; Mohamed, S.; and Vedaldi, A. 2014. Describing textures in the wild. In *Proc. of CVPR*.
- Cubuk, E. D.; Zoph, B.; Shlens, J.; and Le, Q. V. 2020. Randaugment: Practical automated data augmentation with a reduced search space. In *Proc. of CVPR*.
- Dosovitskiy, A.; Beyer, L.; Kolesnikov, A.; Weissenborn, D.; Zhai, X.; Unterthiner, T.; Dehghani, M.; Minderer, M.; Heigold, G.; Gelly, S.; Uszkoreit, J.; and Houlsby, N. 2020. An Image is Worth 16x16 Words: Transformers for Image Recognition at Scale. *ArXiv*, abs/2010.11929.
- Dunlap, L.; Umino, A.; Zhang, H.; Yang, J.; Gonzalez, J. E.; and Darrell, T. 2023. Diversify Your Vision Datasets with Automatic Diffusion-Based Augmentation. *ArXiv*, abs/2305.16289.
- Fei-Fei, L.; Fergus, R.; and Perona, P. 2004. Learning Generative Visual Models from Few Training Examples: An Incremental Bayesian Approach Tested on 101 Object Categories. *2004 Conference on Computer Vision and Pattern Recognition Workshop*, 178–178.
- He, K.; Zhang, X.; Ren, S.; and Sun, J. 2016. Deep residual learning for image recognition. In *Proc. of CVPR*.
- He, R.; Sun, S.; Yu, X.; Xue, C.; Zhang, W.; Torr, P. H. S.; Bai, S.; and Qi, X. 2022. Is synthetic data from generative models ready for image recognition? *ArXiv*, abs/2210.07574.
- Holtzman, A.; Buys, J.; Forbes, M.; and Choi, Y. 2019. The Curious Case of Neural Text Degeneration. *arXiv preprint arXiv:1904.09751*.
- Jia, C.; Yang, Y.; Xia, Y.; Chen, Y.-T.; Parekh, Z.; Pham, H.; Le, Q. V.; Sung, Y.-H.; Li, Z.; and Duerig, T. 2021. Scaling up visual and vision-language representation learning with noisy text supervision. In *Proc. of ICML*.
- Krause, J.; Deng, J.; Stark, M.; and Fei-Fei, L. 2013. Collecting a large-scale dataset of fine-grained cars.
- Krizhevsky, A. 2009. Learning multiple layers of features from tiny images.
- Li, A. C.; Prabhudesai, M.; Duggal, S.; Brown, E. L.; and Pathak, D. 2023. Your Diffusion Model is Secretly a Zero-Shot Classifier. *ArXiv*, abs/2303.16203.
- Li, B.; Hou, Y.; and Che, W. 2022. Data augmentation approaches in natural language processing: A survey. *AI Open*, 3.
- Li, B.; Wu, F.; Lim, S.-N.; Belongie, S. J.; and Weinberger, K. Q. 2021. On feature normalization and data augmentation. In *Proc. of CVPR*.
- Li, J.; Li, D.; Xiong, C.; and Hoi, S. C. H. 2022. Blip: Bootstrapping language-image pre-training for unified vision-language understanding and generation. *arXiv preprint arXiv:2201.12086*.
- Loshchilov, I.; and Hutter, F. 2018. Decoupled Weight Decay Regularization. In *Proc. of ICLR*.
- Meng, Y.; Huang, J.; Zhang, Y.; and Han, J. 2022. Generating Training Data with Language Models: Towards Zero-Shot Language Understanding. *ArXiv*, abs/2202.04538.
- Minaee, S.; Boykov, Y.; Porikli, F. M.; Plaza, A. J.; Kehtarnavaz, N.; and Terzopoulos, D. 2021. Image segmentation using deep learning: A survey. *PAMI*.

- Nilsback, M.-E.; and Zisserman, A. 2008. Automated flower classification over a large number of classes. In *Proc. of ICVGIP*.
- Parkhi, O. M.; Vedaldi, A.; Zisserman, A.; and Jawahar, C. V. 2012. Cats and dogs. In *Proc. of CVPR*.
- Paszke, A.; Gross, S.; Massa, F.; Lerer, A.; Bradbury, J.; Chanan, G.; Killeen, T.; Lin, Z.; Gimelshein, N.; Antiga, L.; Desmaison, A.; Köpf, A.; Yang, E.; DeVito, Z.; Raison, M.; Tejani, A.; Chilamkurthy, S.; Steiner, B.; Fang, L.; Bai, J.; and Chintala, S. 2019. PyTorch: An Imperative Style, High-Performance Deep Learning Library. In *Proc. of NeurIPS*.
- Radford, A.; Kim, J. W.; Hallacy, C.; Ramesh, A.; Goh, G.; Agarwal, S.; Sastry, G.; Askell, A.; Mishkin, P.; Clark, J.; Krueger, G.; and Sutskever, I. 2021. Learning transferable visual models from natural language supervision. In *Proc. of ICML*.
- Rombach, R.; Blattmann, A.; Lorenz, D.; Esser, P.; and Ommer, B. 2022. High-resolution image synthesis with latent diffusion models. In *Proc. of CVPR*.
- Schuhmann, C.; Beaumont, R.; Vencu, R.; Gordon, C.; Wightman, R.; Cherti, M.; Coombes, T.; Katta, A.; Mullis, C.; Wortsman, M.; Schramowski, P.; Kundurthy, S.; Crowson, K.; Schmidt, L.; Kaczmarczyk, R.; and Jitsev, J. 2022. LAION-5B: An open large-scale dataset for training next generation image-text models. *ArXiv*, abs/2210.08402.
- Shen, T.; Lei, T.; Barzilay, R.; and Jaakkola, T. 2017. Style transfer from non-parallel text by cross-alignment. *Advances in neural information processing systems*, 30.
- Shipard, J.; Wiliem, A.; Thanh, K. N.; Xiang, W.; and Fookes, C. 2023. Diversity is Definitely Needed: Improving Model-Agnostic Zero-shot Classification via Stable Diffusion.
- Wang, Z.; Yu, A. W.; Firat, O.; and Cao, Y. 2021a. Towards Zero-Label Language Learning. *ArXiv*, abs/2109.09193.
- Wang, Z.; Yu, J.; Yu, A. W.; Dai, Z.; Tsvetkov, Y.; and Cao, Y. 2021b. SimVLM: Simple Visual Language Model Pre-training with Weak Supervision. In *Proc. of ICLR*.
- Wolf, T.; Debut, L.; Sanh, V.; Chaumond, J.; Delangue, C.; Moi, A.; Cistac, P.; Rault, T.; Louf, R.; Funtowicz, M.; Davison, J.; Shleifer, S.; von Platen, P.; Ma, C.; Jernite, Y.; Plu, J.; Xu, C.; Scao, T. L.; Gugger, S.; Drame, M.; Lhoest, Q.; and Rush, A. M. 2020. Transformers: State-of-the-Art Natural Language Processing. In *Proceedings of the 2020 Conference on Empirical Methods in Natural Language Processing: System Demonstrations*. Online: Association for Computational Linguistics.
- Xu, X.; Wu, C.; Rosenman, S.; Lal, V.; Che, W.; and Duan, N. 2022. Bridge-Tower: Building Bridges Between Encoders in Vision-Language Representation Learning. *arXiv preprint arXiv:2206.08657*.
- Yang, S.; Xiao, W.-T.; Zhang, M.; Guo, S.; Zhao, J.; and Furao, S. 2022. Image Data Augmentation for Deep Learning: A Survey. *arXiv preprint arXiv:2204.08610*.
- Ye, J.; Gao, J.; Li, Q.; Xu, H.; Feng, J.; Wu, Z.; Yu, T.; and Kong, L. 2022. ZeroGen: Efficient Zero-shot Learning via Dataset Generation. In *Conference on Empirical Methods in Natural Language Processing*.
- Yun, S.; Han, D.; Oh, S. J.; Chun, S.; Choe, J.; and Yoo, Y. J. 2019. Cutmix: Regularization strategy to train strong classifiers with localizable features. In *Proc. of ICCV*.
- Zagoruyko, S.; and Komodakis, N. 2016. Wide Residual Networks. In *Proc. of BMVC*.
- Zhang, Y.; Zhou, D.; Hooi, B.; Wang, K.; and Feng, J. 2022. Expanding Small-Scale Datasets with Guided Imagination. *arXiv preprint arXiv:2211.13976*.
- Zhong, Z.; Zheng, L.; Kang, G.; Li, S.; and Yang, Y. 2020. Random erasing data augmentation. In *Proc. of AAAI*.

A Combined Experiments with CutMix

As mentioned in Sec. 4.3, SGID can be combined with other image augmentation baselines and further improves the overall performance. We do not conduct combined experiments for SGID+DiverseCaption or SGID+InstructPix2Pix since they are the variants of SGID. We introduce the combined experimental results between SGID and CutMix in this section, as shown in Appendix Table 7.

We explore applying CutMix based on SGID, *i.e.*, conducting the CutMix transformation based on the augmented images of SGID. We find the combined method achieves the most obvious performance gain on Resnet-50 (from scratch). Specifically, “SGID & CutMix” exceeds both CutMix and SGID by 11.25% and 1.99%. The significant performance gains further prove that our SGID brings good diversity by diffusion models and preserves the essential original semantics by semantic guidance. This paradigm still benefits the perturbation-based CutMix on ResNet-50 (from scratch). As for Vit (ImageNet-21k) and CLIP-ViT (LAION-2B), “SGID & CutMix” achieves slightly better or comparable results to CutMix, and we will explore the reason in the future.

B Image Filters

We explore the effects of image filters for potential better performance. Three categories of image filters are conducted. (1) Label Filter: we use CLIP (Radford et al. 2021) to predict whether the augmented image is related to the groundtruth label or not. For example, in *CIFAR-100*, we provide the list of textual labels including “a photo of an airplane”, “a photo of a bird”, “a photo of a horse”, ..., “a photo of a truck”. All images under the *bird* label that are not classified as “a photo of a bird” are removed. (2) Prompt Filter: we use CLIP to calculate the similarity between each single augmented image and the prompt used to generate this augmented image. The average similarity under each label is calculated and we apply it as the threshold. The augmented images with similarities lower than the threshold will be removed. Thus, images of some proportions will be removed in each label. (3) Original Image Filter: we calculate the similarity between each single augmented image and the original image. The average similarity under each label is calculated and we apply it as the threshold. The augmented images with similarities lower than the threshold will be removed. Thus, images of some proportions will be removed in each label. We conduct this experiment for analysis and we have no objection to potential further improvements with more carefully designed filters.

We conduct experiments on ResNet-50 (from scratch), as shown in Appendix Table 7. The *Label Filter* outperforms SGID on CIFAR-100 and CIFAR-10, which we attribute that the datasets are coarse-grained and the image size is very small, thus a filter tends to improve the performance. The *Prompt Filter* outperforms SGID on Pets and DTD, which we attribute that the generated captions bring more vivid and detailed semantic information than the labels, thus the prompt filter performs the best. The *Original Image Filter* does not achieve performance gain on each dataset, which

	CIFAR-100-S	Cars	Pets	DTD
Backbone	39.90	82.15	49.19	14.57
+ GIF	61.10 ($\times 5$)	75.70 ($\times 20$)	73.40 ($\times 30$)	43.40 ($\times 20$)
+ SGID	65.20 ($\times 2$)	88.28 ($\times 1$)	76.15 ($\times 1$)	45.12 ($\times 2$)

Table 5: Comparison between GIF and SGID. ($\times n$) indicates that the augmented data is n times the original data.

we attribute that the images filtered out through the original image are diverse ones that have a positive effect on image classification. That is, our SGID tends to have a very limited amount of low-level failure. SGID achieves the best performance on average. We attribute that our method introduces semantic guidance to preserve the semantic consistency from the original images, and this confirms the quality of the augmented image.

C Analysis on Two Strong Baselines

To show the effectiveness of SGID, we provide a detailed analysis with two strong baselines across three backbones from three perspectives. We choose the perturbation-based RandAugment as well as the generative Text2Img as our focus. The results are shown in Fig. 6-7. (1) SGID vs the backbones: SGID surpasses all three backbones on all datasets, specifically, the performance gain on ResNet-50 (from scratch) is the most obvious, and we still see improvement on CLIP-VIT (LAION-2B), whose pre-training data is almost identical to Stable Diffusion. This shows the effectiveness of the paradigm of SGID. (2) SGID vs the strong baselines: Our method outperforms two strong baseline models on the vast majority of all datasets. This conclusion is valid on all three backbones. This is because SGID brings good diversity by diffusion models and preserves semantic consistency through semantic guidance. It balances image diversity and semantic consistency, and archives better performance than strong perturbation-based and generative baselines. (3) SGID can be combined with other baselines for further performance improvement, and this conclusion holds for both perturbation-based baselines and generative baselines. For example, both *SGID & RandAugment* and *Text2Img & SGID* outperforms the baselines themselves on all three backbones. Consistent and significant performance gains further prove our SGID not only preserves the essential semantics of the original images while bringing good diversity, but also benefits the baselines.

D Comparison with Image Variation

We compare our approach with GIF (Zhang et al. 2022), an image variation method conditioned on CLIP image embeddings.¹¹ They perturb and optimize the latent features of the original image and input them to a pre-trained image generation model to generate the image. However, they use the original images only as the input. The image labels are only used during optimizing the training loss, instead of used for constructing the textual prompt along with image captions

¹¹We introduce it in Appendix Sec. G

as input, *i.e.*, as a **explicit** semantic guidance for image-to-image generation in SGID. Moreover, their methods require additional training on the pre-trained image generation models, and more times of expansion (usually 5-30 times) are required to achieve a boost on the datasets.

We provide a fair comparison with GIF based on Stable Diffusion and ResNet-50 (from scratch) in Appendix Table 5. Since GIF does not provide their code or models, in Appendix Table 5, we provide the results of “Backbone” from our experiments. “CIFAR-100-S” indicates 100-shot of CIFAR-100. Experiments show that GIF underperforms our proposed SGID, which we attribute to the performance fluctuations of CLIP image embedding on different datasets (Radford et al. 2021) and the optimization difficulty of GIF. Unlike optimizing the image features with label constraints, SGID proposes to construct prompts with golden labels and captions to better guide the image-to-image generation process.

This provides more precise and explicit semantic information than the implicit semantic constraints via optimizing losses based on labels. Significant improvements with a smaller number of dataset expansion multiples (up to 2 times on CIFAR-100-S) prove the effectiveness of SGID. Besides, our method is also applicable to larger datasets (such as CIFAR-10 and CIFAR-100) and require no additional training on the pre-trained image generation models. The results also show that SGID preserves semantic consistency by semantic guidance, which is important for image classification. Our SGID obtains obvious performance gain by balancing image diversity and semantic consistency.

E Image-Text Pre-trained Models

Benefiting from vision-language pre-training on large-scale image-text pairs (Jia et al. 2021; Changpinyo et al. 2021), there has been a lot of work successfully unifying text and image in the united space (Cho et al. 2021; Wang et al. 2021b; Xu et al. 2022).

Overall, there are three kinds of vision-language pre-trained models used in this paper: (1) **CLIP** (Radford et al. 2021) consists of a text encoder and an image encoder that encodes both images and texts and successfully bridges the feature space between language and vision. We use it to measure the similarity between images and texts. (2) **BLIP** (Li et al. 2022), an encoder-decoder model jointly pre-trained with three vision-language objectives: image-text contrastive learning, image-text matching, and image-conditioned language modeling, achieves great results on a wide range of vision-language tasks such as image captioning and visual question answering. (3) **Stable Diffusion** (Rombach et al. 2022), an image generation model pre-trained on LAION-2B (Schuhmann et al. 2022), captures the essential image information by compressing images from the pixel space to the latent space, and gradually adding Gaussian noise for the diffusion process. The CLIP text encoder converts the text description into the condition for the denoising process, and the image decoder decodes the denoised image into the final image.

In this paper, **the reason why we choose Stable Diffusion as the image generation model** is that it is a widely

used and highly effective open-source *image-to-image* generation model that supports *semantic injection* and noise rate tuning, which perfectly matches our approach (see Sec. 3). Moreover, the diffusion and conditional denoising process provides *good diversity* for image generation and achieves good results on some downstream tasks including image generation. The significant performance of SGID also justifies the choice of Stable Diffusion (see Sec. 4).

F Case Study of DA Methods

We show augmented images of SGID and other image augmentation baselines on the following datasets, including CIFAR-100, CIFAR-10, Caltech101, Flowers102, OxfordPets, and DTD. The results are shown in Figure 8 - Figure 13.

G Other generative DA methods

GIF (Zhang et al. 2022) optimizes the latent features of the original image in the semantic space and decodes the features into augmented images with new content (Zhang et al. 2022). We compare SGID with it in Appendix Sec. 5. *ALIA* (Dunlap et al. 2023) generates captions for each original image, and use the captions across the datasets to language models and summarize them into some descriptions like image background. They use these descriptions as the captions or edit instructions to edit each original image. They conduct experiments on fine-grained datasets. We take the variants of this method as our baselines (SGID+DiverseCaption and SGID+InstructPix2Pix) because we have coarse-grained datasets and we summarize captions on each label, which is a more general setting.

H Datasets and Baselines

Datasets: We evaluate the effectiveness of our proposed method on seven commonly used datasets, including three coarse-grained object classification datasets: CIFAR-10 (Krizhevsky 2009), CIFAR-100 (Krizhevsky 2009), Caltech101 (Cal101) (Fei-Fei, Fergus, and Perona 2004), and four fine-grained object classification datasets: Stanford Cars (Cars) (Krause et al. 2013), Flowers102 (Flowers) (Nilsback and Zisserman 2008), OxfordPets (Pets) (Parkhi et al. 2012) and texture classification (Cimpoi et al. 2014) (DTD). Some other details are shown in Appendix Table 8.

I Implementation Details

Image Generation We apply nucleus sampling and beam search to respectively generate 10 captions by BLIP. The caption length is between 5 and 20. As for nucleus sampling, we use $p = 0.9$ by default as it is considered to be able to generate both fluent and diverse texts (Li et al. 2022). As for beam search, we use $num.beams = 3$ by default. The default “CLIP-ViT-B/32” model is used for calculating image-text similarity. We apply the pre-trained “stable-diffusion-v1-5” model and generate one augmented

		CIFAR-100	CIFAR-10	Cal101	Cars	Flowers	Pets	DTD	Avg.
ResNet-50 (from scratch)	Backbone (He et al. 2016)	75.12	94.81	47.38	82.26	33.02	50.30	19.85	57.53
	+ CutMix (Yun et al. 2019)	<u>77.56</u>	<u>95.52</u>	49.28	83.55	33.35	51.21	20.14	58.66
	+ SGID (Ours)	75.72	95.48	<u>59.17</u>	<u>88.53</u>	45.61	73.71	<u>37.19</u>	<u>67.92</u>
	+ SGID & CutMix	77.81	95.74	61.75	90.50	46.57	75.82	41.15	69.91
ViT (ImageNet-21k)	Backbone (Dosovitskiy et al. 2020)	89.86	98.61	91.20	82.99	95.70	92.04	71.22	88.80
	+ CutMix (Yun et al. 2019)	89.94	98.67	91.77	84.20	96.53	92.45	71.32	89.27
	+ SGID (Ours)	92.66	98.96	93.91	86.73	<u>97.16</u>	93.38	73.35	90.88
	+ SGID & CutMix	<u>91.86</u>	<u>98.85</u>	94.20	87.45	97.66	<u>92.94</u>	<u>73.29</u>	90.89
CLIP-ViT (LAION-2B)	Backbone (Cherti et al. 2022)	85.89	95.04	92.96	85.13	91.46	93.69	65.81	87.14
	+ CutMix (Yun et al. 2019)	85.98	95.20	93.85	85.43	91.64	<u>94.01</u>	66.20	87.47
	+ SGID (Ours)	86.53	95.66	<u>94.29</u>	87.19	<u>92.04</u>	<u>93.98</u>	<u>66.25</u>	<u>87.99</u>
	+ SGID & CutMix	<u>86.19</u>	<u>95.34</u>	94.46	<u>86.49</u>	92.33	94.55	66.73	88.01

Table 6: The results of the combined model with CutMix on three backbones, *i.e.*, conducting the CutMix transformation based on the augmented images of SGID.

		CIFAR-100	CIFAR-10	Cal101	Cars	Flowers	Pets	DTD	Avg.
ResNet-50 (from scratch)	Backbone (He et al. 2016)	75.12	94.81	47.38	82.26	33.02	50.30	19.85	57.53
	+ SGID (Ours)	<u>75.72</u>	<u>95.48</u>	59.17	88.53	45.61	73.71	<u>37.19</u>	67.92
	+ Label Filter	76.23	95.93	58.69	87.56	<u>44.22</u>	<u>75.01</u>	32.71	67.19
	+ Prompt Filter	75.29	95.44	<u>57.37</u>	86.02	43.75	75.47	38.99	<u>67.48</u>
	+ Original Image Filter	75.16	95.26	53.69	86.76	40.88	68.33	36.97	65.29

Table 7: The performance of three categories of image filters.

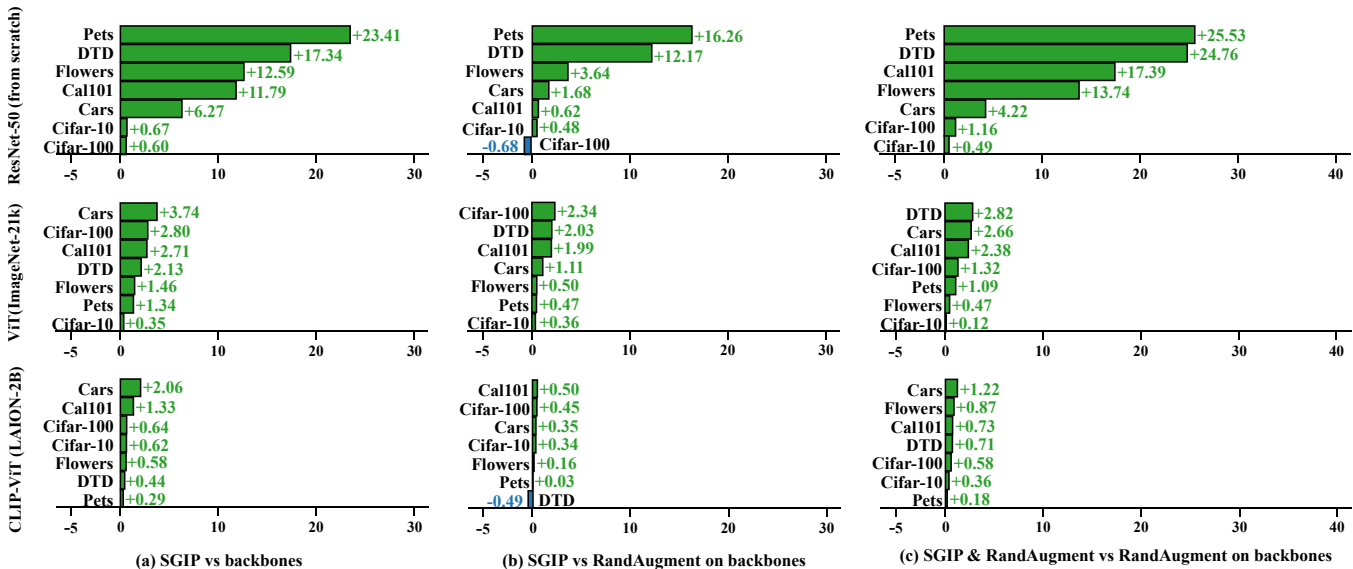


Figure 6: SGID outperforms not only all backbones but also the generative baseline Text2Img. Moreover, SGID can further improve the performance of Text2Img by combining naturally with it.

image for each original image.¹² The *denoising_steps* is set as 100 for higher quality. Empirically, we take $f(s^*) = -4 \cdot (s^*)^2 + 2 \cdot s^* + 1$ as the guidance mapping function. We select the noise rate $n \in [0, 1]$.¹³ As for prompt weight-

¹²SD v1-5 is mainly pre-trained on LAION-2B (Schuhmann et al. 2022).

¹³The larger n brings more variation. We choose n from $\{0.3, 0.5, 0.7\}$ to preserve image semantics and bring explicit

ing. We assign a weight of 1.50 to the labels because it carries more accurate information for the original image, and a weight of 0.90 to the caption to reduce the interference caused by the potential low-quality captions. We provide more details on training image classification models in Appendix Sec. I.

Image Classification: We train ResNet-50 (from scratch)

changes in the background, position, etc.

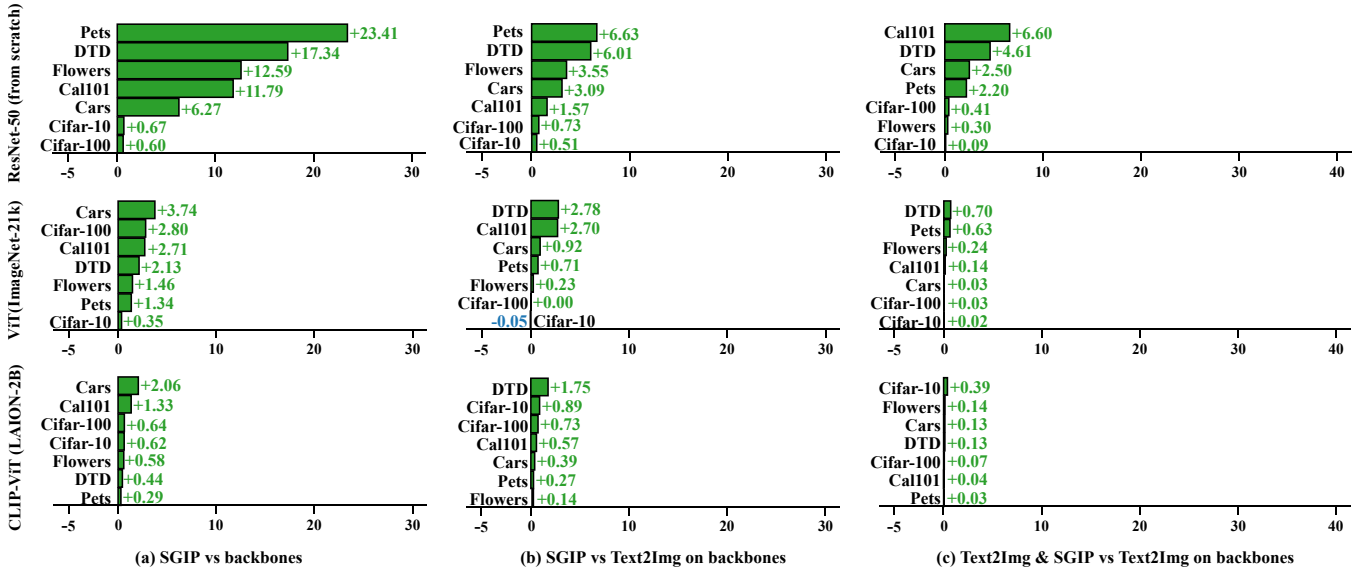


Figure 7: SGID outperforms not only all backbones but also the best perturbation-based baseline RandAugment. Moreover, SGID can further improve the performance of RandAugment by combining naturally with it.

Dataset	Image Label Example	Label Guidance	Caption Guidance			Prompt Weighting
			Beam	Nucleus	CLIP	
CIFAR-100	forest, fox, bed	✓	✗	✓	✗	✓
CIFAR-10	airplane, bird, ship	✓	✗	✗	✓	✓
Call101	anchor, cellphone, pyramid	✓	✗	✓	✗	✗
Cars	Acura_Integra_Type_R_2001, AM_General_Hummer_SUV_2000	✓	✗	✗	✗	✗
Flowers	moon orchid, sword lily	✓	✗	✗	✓	✓
Pets	abyssinian, shiba inu	✓	✓	✗	✗	✗
DTD	banded, zigzagged	✓	✗	✗	✓	✓

Table 8: Detailed experimental settings on label guidance, caption guidance and prompt weighting.

from scratch for 300 epochs. The learning rate starts from 0.1 and is divided by 10 after the 150th and 225th epochs. The batch size is set to 256. We use the SGD optimizer, and the momentum, weight decay are set to 0.9 and $5e-4$. As for the pre-trained ViT (ImageNet-21k) and CLIP-ViT (LAION-2B), we use the framework and settings provided by HuggingFace (Wolf et al. 2020) and OpenCLIP (Cherti et al. 2022). On the CIFAR-10 and CIFAR-100, the learning rate and training epoch are set to $5e-5$ and 3. On the other datasets, we follow (Dosovitskiy et al. 2020) and choose the learning rate based on the best performances among $\{1e-4, 3e-4, 1e-3, 3e-3, 5e-5\}$ and the training epoch is set to 15. All models are trained with the basic image transform methods: randomly performs horizontal flips and, for ResNet-50 (from scratch), takes a random resized crop with 32×32 on CIFAR-10 and CIFAR-100 datasets from images padded by 4 pixels on each side, 224×224 on the other datasets. Models are developed with PyTorch (Paszke et al. 2019). All experiments are conducted with NVIDIA A100 40GB and NVIDIA A100 80GB. More implementation details can be found in Appendix Sec. I.

We adopt three visual backbones for image classifi-

cation, including ResNet-50 (from scratch) (He et al. 2016), WideResNet-28-10 (scratch) (Zagoruyko and Komodakis 2016), ViT (ImageNet-21k) (*vit-base-patch16-224-in21k*; (Dosovitskiy et al. 2020)), and CLIP-ViT (LAION-2B) (Schuhmann et al. 2022). CLIP-ViT (LAION-2B) is pre-trained on LAION-2B (Schuhmann et al. 2022), its base model is ViT-B/32, and the amount of samples seen is 34B. Since “stable-diffusion-v1-5” we apply in this paper is pre-trained on LAION-2B and subset of “laion-aesthetics v2 5+” (600M), the pre-trained source of Stable Diffusion and CLIP-ViT (LAION-2B) are highly similar, thus CLIP-ViT (LAION-2B) is a strong backbone that demonstrates the performance of SGID. Among different DA methods, in order to ensure the fairness of the experiments, a grid search was performed with a fixed seed in the same hyperparameter search space, and the best result of each method is reported. We develop and experiment based on the Pytorch (Paszke et al. 2019) framework. All experiments are conducted with NVIDIA A100.

As for ResNet-50 (from scratch) and WideResNet-28-10 (scratch), we apply basic image transforms, including random horizontal flips and a random resized crop with 32×32

on CIFAR-10 and CIFAR-100 datasets (images are padded by 4 pixels on each side), and 224×224 on other datasets. We train these models from scratch for 300 epochs. Following (Zhong et al. 2020), the learning rate starts from 0.1 and is divided by 10 after the 150th and 225th epoch. The batch size is set to 256 for ResNet-50 (from scratch), and 64 for WideResNet-28-10 (scratch). We use the SGD optimizer, and the momentum, weight decay are set to 0.9 and $5e-4$ for both backbones.

As for ViT (ImageNet-21k), we use the pre-trained <https://huggingface.co/google/vit-base-patch16-224-in21k> *vit-base-patch16-224-in21k* model and the image classification <https://github.com/huggingface/transformers/tree/main/examples/pytorch/image-classificationframework> provided by HuggingFace (Wolf et al. 2020). Basic image transforms are applied, including random horizontal flips and a random resized crop with 224×224 to match the input dimensions of the pre-trained *vit-base-patch16-224-in21k* model on all datasets. During model training, the batch size is set to 64 and the AdamW (Loshchilov and Hutter 2018) optimizer is used. On CIFAR-10 and CIFAR-100, we use the default parameters from the framework, *i.e.*, the learning rate and training epoch are set to $5e-5$ and 3. On the other datasets, we follow (Dosovitskiy et al. 2020) and choose the learning rate based on the best performances among $\{1e-4, 3e-4, 1e-3, 3e-3\}$ and the training epoch is set to 15.

The hyper-parameters of baseline methods are as follows:

- For Random Erasing, we follow the <https://github.com/zhunzhong07/Random-Erasing> official implementation of (Zhong et al. 2020) ($p = 0.5$, $s_h = 0.4$ and $r_1 = 0.3$);
- For CutMix, we follow the <https://github.com/clovaai/CutMix-PyTorch> official implementation of (Yun et al. 2019) ($\alpha = 1$, cutmix probability is 0.5);
- For RandAugment, we use <https://github.com/pytorch/vision/blob/main/torchvision/transforms/autoaugment.pytorchvision.transforms.RandAugment> provided by PyTorch without changing any default parameters ($N = 2$, $M = 9$);
- For MoEx, we follow the <https://github.com/Boyiliee/MoEx> official implementation of (Li et al. 2021) ($\lambda = 0.5$, $p = 0.25$, PONO normalization).

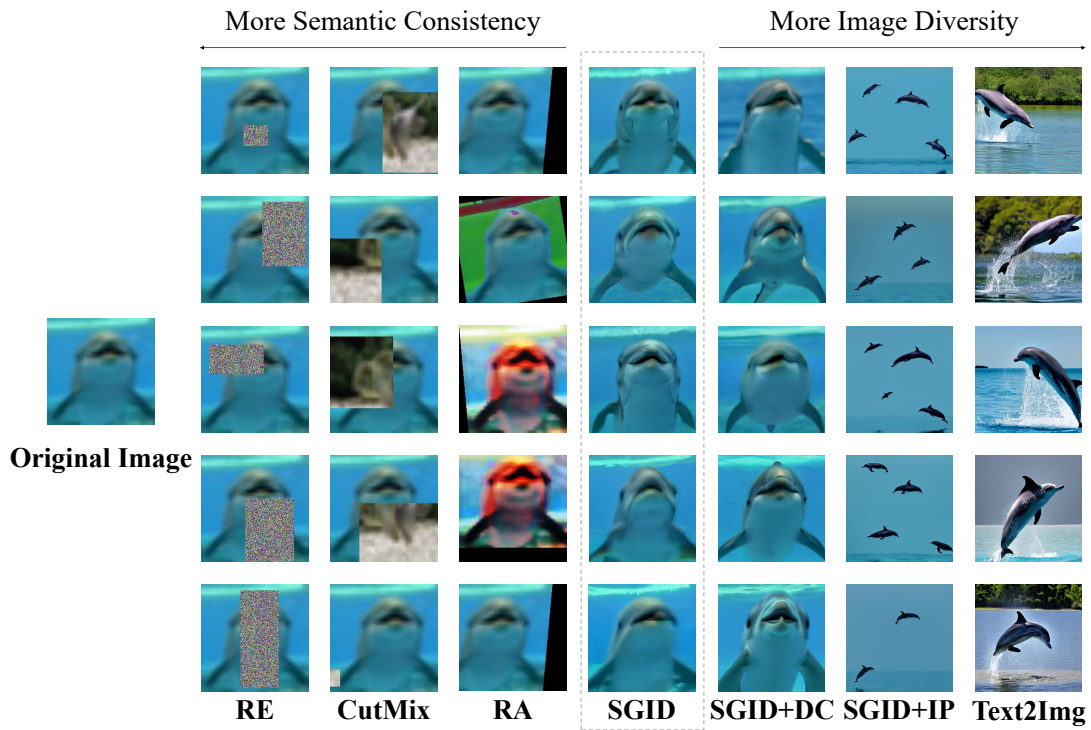


Figure 8: Augmented images by SGID and other DA baselines on CIFAR-100.

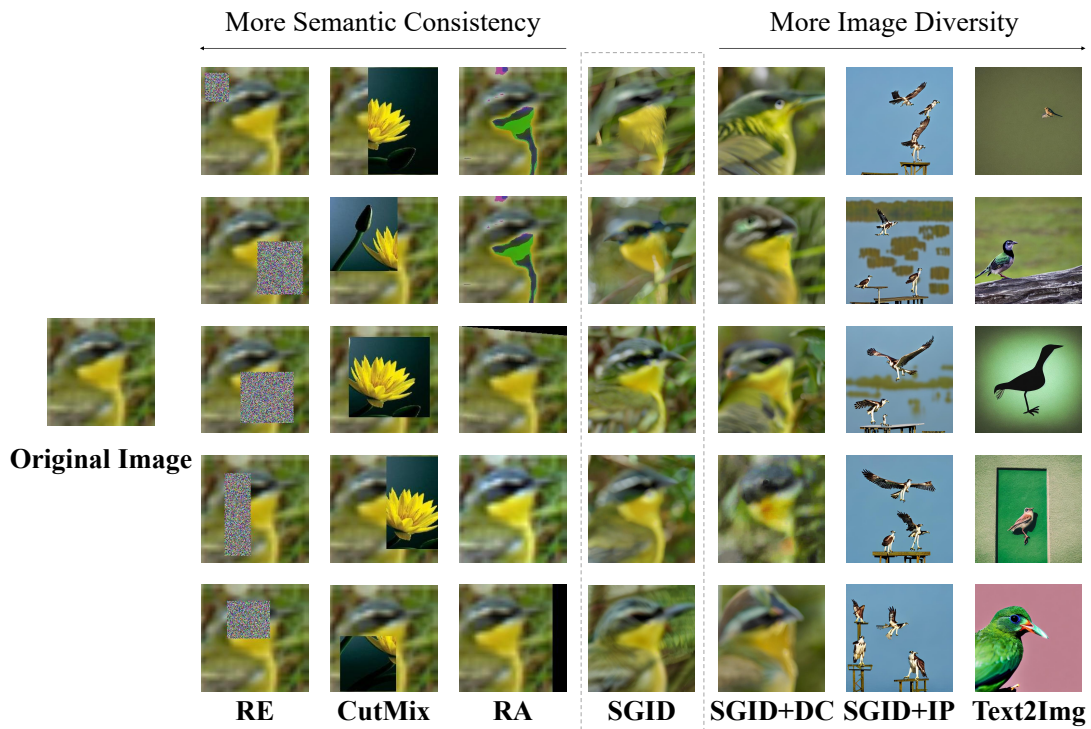


Figure 9: Augmented images by SGID and other DA baselines on CIFAR-10.

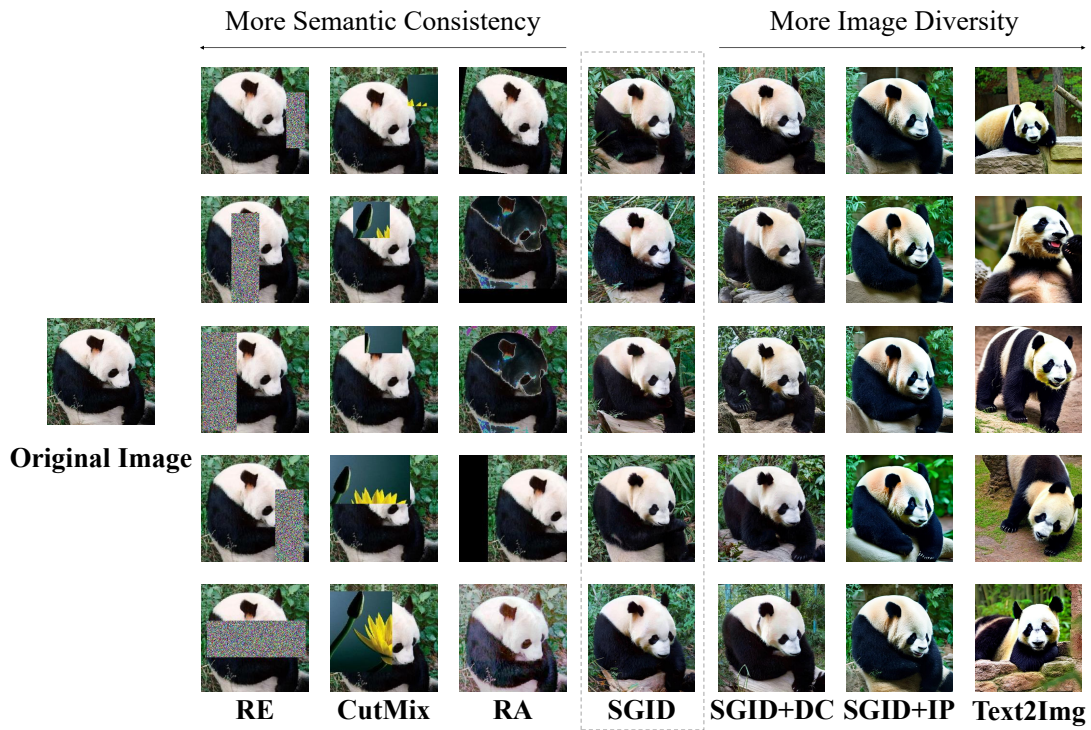


Figure 10: Augmented images by SGID and other DA baselines on Caltech101.

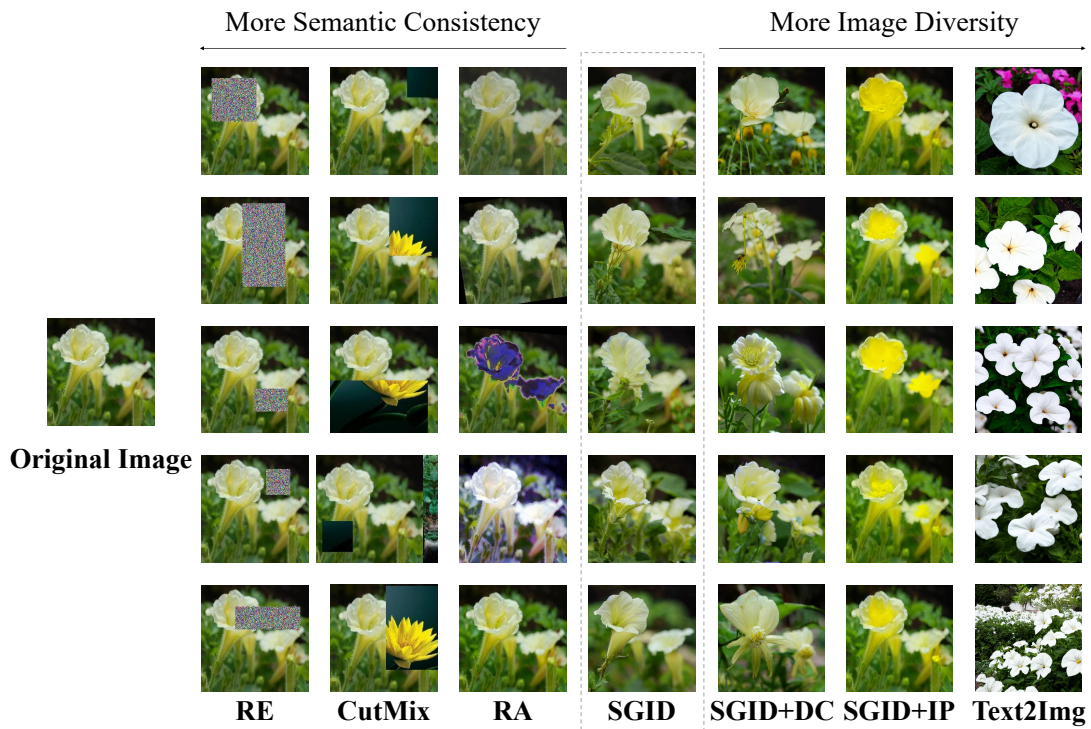


Figure 11: Augmented images by SGID and other DA baselines on Flowers102.



Figure 12: Augmented images by SGID and other DA baselines on OxfordPets.

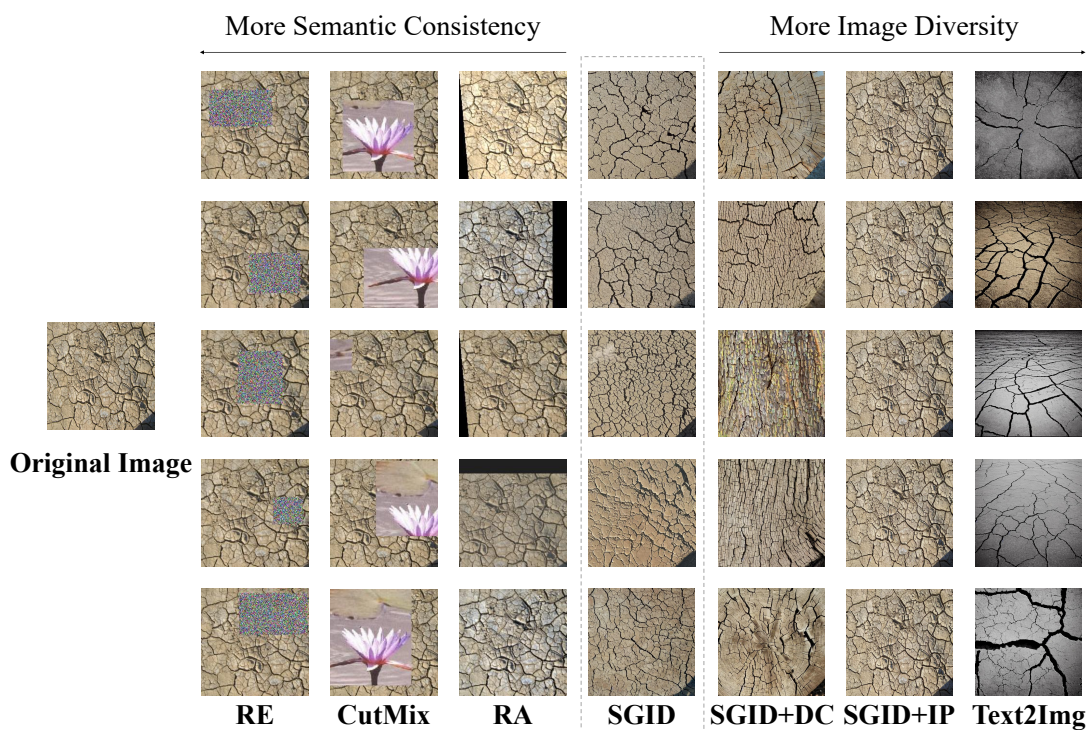


Figure 13: Augmented images by SGID and other DA baselines on DTD.